ELSEVIER

Chemical Engineering Journal 131 (2007) 49–58

Chemical Engineering Journal

www.elsevier.com/locate/cej

Hydrodynamic and mass transfer in a new co-current two-phase flow gas–liquid contactor

C. Sanchez [a,b,*], A. Couvert [a], A. Laplanche [a], C. Renner [b]

[a] *CNRS UMR 6226 – ENSCR, Avenue du Général Leclerc, 35700 Rennes, France*

[b] *ANJOU RECHERCHE – VEOLIA ENVIRONNEMENT, Chemin de la Digue, BP76, 78603 Maisons-Laffitte, France*

Received 11 May 2006; received in revised form 1 December 2006; accepted 4 December 2006

Abstract

This work presents hydrodynamic and mass transfer performances of a new gas–liquid reactor, named CoReC. Compared to conventional gas–liquid contactors with a gas continuous phase like packed towers (PT), the CoReC presents the advantage to be a small sized device. Experiments were carried out to quantify pressure drop ΔP, volumetric interfacial area a, and liquid side mass transfer coefficients ($k_L a$ and k_L) for superficial gas and liquid velocities varying from 5.6 to 28 m s^{-1} and 0.016 to 0.055 m s^{-1}, respectively. Different flow configurations (vertical upward (VU), vertical downward (VD) and horizontal (H)) were tested. The results were compared to a previous study lead on Lightnin SM. Pressure drop ΔP inside the CoReC, ranging from 500 up to 20,000 Pa m^{-1}, was found lower than the one generated by classical SM. Volumetric interfacial area a and mass transfer coefficient $k_L a$, respectively reaching values of 2800 m^2 m^{-3} and 0.22 s^{-1}, were found higher than those encountered in SM, and far better than those measured in PT. Moreover, it has been shown that the flow configuration is an important parameter to take into account. VD configuration appeared to be the most economically acceptable with advantageous interfacial areas, high mass transfer coefficients and the lowest pressure drops if compared to VU and H configurations.

Keywords: Absorption; Chemical processes; Gas continuous phase; Gas–liquid contacting; Hydrodynamics; Mass transfer; Scrubber; Static mixer

1. Introduction

The purification of gaseous wastes containing volatile organic compounds (VOCs) presents special difficulties because of the large gas volumes and the low pollutant concentrations to be treated. During the last decades, many processes have been designed in order to clean these kinds of polluted atmospheres. Among them, absorption processes allow the transfer of a pollutant from the gas phase to a liquid phase, with or without any chemical reaction. The goal of these gas–liquid devices is to transfer VOCs from large gas volumes with low concentrations of pollutants, to small liquid volumes. A wide range of absorption apparatuses is available on the market: stirred tanks, bubble columns, packed-bed columns, plate-columns, static or dynamic mixers. The choice of the best absorption process is difficult, taking into account the important number of variables that have to be considered in a scrubber design.

PT are encountered in most of industries and remain one of the most effective and economic process for gas–liquid absorption processes. Nevertheless, better and better performances are required, in smaller and smaller cost effective units. This permanent demand leads researchers to look for better-designed and higher efficient processes. Many of them have focused their attention on improving the packing inside the columns, aiming at increasing mass transfer capacities, and decreasing pressure drops. In the last decades, structured packings [1–4,34,35] and static mixers [5–14,31] have gained increased attention because of their properties: high bed void fraction resulting in low pressure drops with excellent gas–liquid contact and distribution [30].

First versions of structured packings were fabricated from metal gauze with specific surface area up to 500 m^2 m^{-3}. Nowadays, structured packings are mostly made of corrugated sheet metals (typically 45° with respect to the horizontal) with specific surface area of about 250 m^2 m^{-3}, metal sheet packings with various surface areas and larger corrugation angle (60°),

* Corresponding author at: CNRS UMR 6226 – ENSCR, Avenue du Général Leclerc, 35700 Rennes, France.

E-mail address: sanchezcelia@yahoo.fr (C. Sanchez).

1385-8947/$ – see front matter © 2007 Elsevier B.V. All rights reserved.
doi:10.1016/j.cej.2006.12.004

Nomenclature

a	volumetric interfacial area (L^{-1})
C	concentration in the liquid phase, in the bulk ($N\,L^{-3}$)
C^*	concentration at the gas–liquid interface ($N\,L^{-3}$)
C_{OH^-}	NaOH liquid concentration ($N\,L^{-3}$)
$D_{(A)L}$	diffusivity of the product A in the liquid used ($L^2\,T^{-1}$)
D_i	internal diameter of the pipe (L)
E	enhancement factor
f	friction factor
G	mass gas flow rate per surface unit ($M\,L^{-2}\,T^{-1}$)
H	Henry constant ($M\,L^2\,N^{-1}\,T^{-2}$)
Ha	Hatta number
I	ionic strength ($N\,L^{-3}$)
k_2	kinetic constant of the reaction between CO_2 and NaOH 1N ($L^3\,N^{-1}\,T^{-1}$)
k_L	liquid side mass transfer coefficient ($L\,T^{-1}$)
k_La	volumetric liquid side mass transfer coefficient (T^{-1})
k_Ga	volumetric gas side mass transfer coefficient ($Pa\,L^3\,T\,N^{-1}$)
L	mass liquid flow rate per surface unit ($M\,L^{-2}\,T^{-1}$)
N	flux of product A transferred ($N\,T^{-1}$)
ΔP	Pressure drop ($M\,L^{-1}\,T^{-2}$)
Q	flow rate ($L^3\,T^{-1}$)
U_S	superficial velocity ($L\,T^{-1}$)
V_r	reaction volume (L^3)
y_{in}	molar fraction of CO_2 in the reactor inlet
y_{out}	molar fraction of CO_2 in the reactor outlet
Z_i	ion valence

Symbols

ρ	density ($M\,L^{-3}$)
ϕ_{CO_2}	CO_2 absorption rate ($L^{-3}\,T^{-1}\,N$)

embossed plates stacked in layers forming open channels, etc. They have been shown to satisfy the growing needs for better efficiency and greater capacity. As an example, when the liquid is the continuous phase, Al Taweel et al. [15] obtained k_La equal to $0.44\,s^{-1}$ in a screen-type static mixer. In the same type of SM, Chen [32] reached interfacial areas of $2200\,m^2\,m^{-3}$. The major drawback in the use of structured packings is their high price per unit volume, which leads to a higher investment cost than for random PT. Therefore, in order to make the process competitive, an accurate design of columns equipped with structured packings is very important for minimising the investment and operating costs.

Most of the studies found in the literature focus on counter-current flow applications. But, when absorbed species react in the liquid phase under a fast irreversible chemical reaction, the co-current flow configuration allows high flexibility [16] and a gain of space, avoiding flooding in the same time. Consequently, the objective of this work was to develop an efficient, low investment and operating cost gas–liquid contactor, able to generate high interfacial areas and good mass transfer coefficients without creating high pressure drop. In this study, pressure drop (energy consumption) and mass transfer parameters (efficiency) were characterised in the CoReC. Different configurations were tested, depending on the flow direction (VD, VU and H). Pressure drop ΔP and mass transfer parameters (a, k_La, k_L, k_Ga) have been measured and correlated to the superficial gas and liquid velocities.

2. Experimental study

2.1. Experimental set-up

A schematic diagram of the experimental set-up is shown in Fig. 1. The CoReC consists of a transparent PVC pipe of 0.32 m length and 0.025 m inner diameter, through which flow patterns as well as the type of dispersion can be observed. The contactor is a new wire mesh packing structure which geometric characteristics are given in Table 1. The overall geometric interfacial area takes the surface offered by the packing itself and by the column wall (which cannot be neglected in a small diameter column) into account. The volume of the contactor is calculated from the length and the inner diameter of the PVC tube.

Whatever the configuration, the gas used in these experiments was over-pressured air, injected upstream of the CoReC. The gas flow rates ranged from 10 to $50\,m^3\,h^{-1}$ (superficial gas velocities from 5.6 to $28\,m\,s^{-1}$). The flow rate is controlled with a rotameter. The pressure drop within the reactor is measured with a manometer. Suitable compounds (CO_2 for the volumetric interfacial area and k_Ga measurements, 2-butanone for the k_La measurement) are introduced with an automatic syringe distributor in the inlet air flow. The liquid phase is injected into the reactor using a centrifugal pump, which distributes it at the inlet of the pipe, such that it circulates in the same direction as the gas flow. The liquid flow rates, measured owing to a flow meter, ranged between 0.0275 and $0.0975\,m^3\,h^{-1}$ (superficial liquid velocities between 0.016 and $0.055\,m\,s^{-1}$).

2.2. Experimental methodology

Experiments were performed for superficial gas and liquid velocities ranging from 5 to $28\,m\,s^{-1}$ and from 0.016 to $0.055\,m\,s^{-1}$, respectively. Temperature is constant and equal to 20 °C. Fluids circulate in co-current flow in the tube. Some liquid and gas samples are picked up (outlet for the liquid phase, inlet and outlet for the gas phase) and analysed.

Table 1
Geometric characteristics of the CoReC

Height (m)	0.32
Internal diameter (m)	0.025
Void fraction (%)	97.5
Geometric surface a_g ($m^2\,m^{-3}$)	170
Volume (m^3)	0.000058

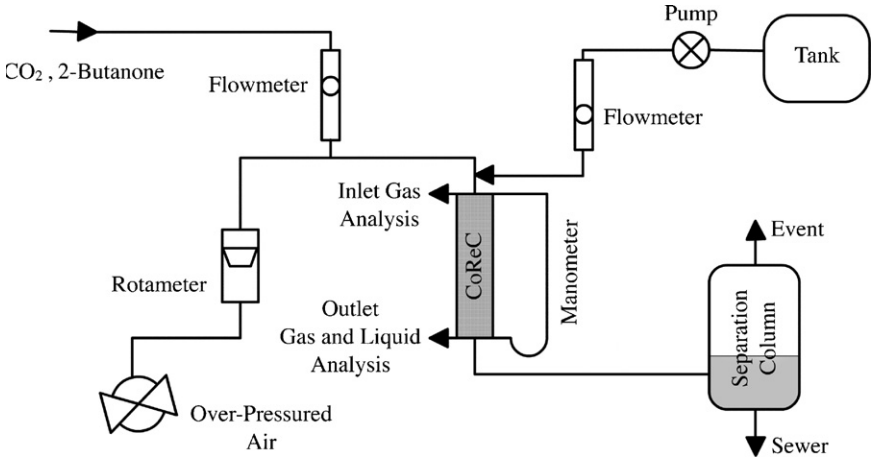

Fig. 1. Scheme of the experimental set-up in vertical downward flow configuration.

2.2.1. Pressure drop ΔP

Pressure drop ΔP is measured with two manometers: the first one is filled with water (for the low pressure drop values) and the second one is filled with mercury (for the high pressure drop values). They are connected just before and after the CoReC and the pressure drop is measured for the different liquid and gas flow rates mentioned previously.

2.2.2. Volumetric interfacial area a

The chemical method used to measure the volumetric interfacial area has been developed by Danckwerts [33], particularly to study mass transfer in random PT. It is based on the measurement of the absorption rate of a gaseous component, which is absorbed and reacts in the liquid phase. As the reaction kinetics and thermodynamic properties are well established, it is possible to deduce the mass transfer characteristics. In the present study, the NaOH–CO_2 system (gas composed of carbon dioxide (CO_2) and liquid aqueous solution of NaOH of different concentrations) has been chosen, mainly because the corresponding reaction kinetics and thermodynamic data can easily be found in the literature.

Within the CoReC, hydroxide ions OH^- are consumed by the absorbed CO_2 according to the mechanism described by the following equations:

$$CO_{2(G)} \leftrightarrow CO_{2(L)} \quad (1)$$

$$CO_{2(L)} + OH^- \leftrightarrow HCO_3^- \quad (2)$$

$$HCO_3^- + OH^- \leftrightarrow CO_3^{2-} + H_2O \quad (3)$$

Eq. (1) corresponds to the CO_2 gas–liquid equilibrium, Eq. (2) the reaction to consider for kinetics since reaction (3) has a much higher rate constant than reaction (2) [17]. In the second reaction, the dependence of the second-order reaction rate constant, k, on the ionic strength I and the temperature T, was studied by Laurent [18]:

$$\log k = 13.4 - \frac{2350}{T} + 0.133I \quad (4)$$

$$\text{With} \quad I = \sum_i \frac{1}{2} C_i Z_i^2 \quad (5)$$

C_i is the concentration of ions in the solution and Z_i is their valence.

The rate constant was calculated at 20 °C, its values are summarised in Table 2. In the present case, hydroxide ions are in large excess and the reaction is fast (Hatta number Ha reaches values up to 50); thus it can be assumed that:

(i) all the absorbed CO_2 is transformed into CO_3^{2-};
(ii) the ratio between the CO_2 partial pressure P_{CO_2} and the Henry's constant, H, is much larger than the CO_2 concentration in the liquid phase;
(iii) the thermodynamic equilibrium is reached at the interface;
(iv) the reaction is of pseudo first-order.

In this case, the specific absorption flux per liquid volume unit Φ_{CO_2} is given by the following equation:

$$\frac{PCO_2}{\Phi CO_2} = \frac{1}{k_G a} + \frac{H}{Hak_L a} = \frac{1}{a}\left[\frac{1}{k_G} + \frac{H}{(\sqrt{DCO_2 k_2 C_{OH^-}})}\right] \quad (6)$$

If we assume that CO_2 molar flux is much less than OH^- molar flux, the global balance Φ_{CO_2} is determined by the following

Table 2
Rate constant of the reaction between CO_2 and NaOH, viscosity of NaOH and CO_2, and diffusivity coefficient in NaOH for NaOH concentration varying from 0.25 to 1 mol L^{-1}

	[NaOH] (mol L^{-1})				
	0.25	0.375	0.5	0.75	1
k (L mol^{-1} s^{-1})	6600	7013	7444	8357	9339
μ_{NaOH} (10^3 Pa s)	1.03	1.06	1.09	1.15	1.22
$D_{(CO_2/NaOH)}$ (10^9 m^2 s^{-1})	1.83	1.74	1.70	1.61	1.53

equation:

$$\Phi_{CO_2} = \frac{Q_G(Y_{out} - Y_{in})}{V_r} \quad (7)$$

Y_{in} and Y_{out} are, respectively, the CO_2 molar fraction at the inlet and outlet. V_r is the reaction volume and Q_G is the molar gas flow rate.

As stated by Wilke and Chang [19], the diffusivity coefficient of CO_2 in NaOH solutions $D_{CO_2/NaOH}$ can be calculated from the diffusivity coefficient of CO_2 in water [17]:

$$D_{(CO_2/water)}\mu_{water} = D_{(CO_2/NaOH)}\mu_{NaOH} \quad (8)$$

$D_{(CO_2/water)} = 1.73 \times 10^{-9}\ m^2\ s^{-1}$ [20]. NaOH viscosity was measured with a Brookfield LVDV-II + CP viscometer and allowed us to calculate the diffusivity coefficient for the different NaOH concentrations studied (Table 2). Considering Eq. (6), if the effective interfacial area, and the gas side mass transfer coefficient are constant along the column, it is possible from the slope of the best linear fit of P_{CO_2}/Φ_{CO_2} versus $[H/(\sqrt{D_{CO_2}k_2C_{OH^-}})]$, to determine the effective interfacial area and from the intercept to deduce k_Ga.

2.2.3. Volumetric liquid side mass transfer coefficient k_La

Volumetric mass transfer coefficient k_La was measured thanks to the implementation of a physical transfer of gaseous 2-butanone in an aqueous phase (water, which pH is adjusted to 7 with NaOH). 2-Butanone has been chosen because of its small solubility (Henry's constant $H = 6.7 \times 10^{-2}$ atm L mol^{-1} at 25 °C). 2-Butanone was injected as a liquid in the gas flow with a syringe distributor, vaporised in it in order to reach a concentration of about 50 mg m^{-3} in the gas phase. In this case, the mass transfer resistance is located in the liquid film, and the 2-butanone liquid concentration at the inlet is zero; then the volumetric mass transfer coefficient can be written as follows (Eq. (9)):

$$k_La = \frac{N}{EV(C^*_{AL,e} - (C^*_{AL,s} - C_{AL,s}))/\ln C^*_{AL,e}/(C^*_{AL,s} - C_{AL,s})} \quad (9)$$

With N is the flux of 2-butanone transferred, V the liquid volume in the contactor, $C_{AL,s}$ the concentration of 2-butanone in the liquid phase at the outlet, $C^*_{AL,e}$ and $C^*_{AL,s}$ the concentration of 2-butanone at the gas–liquid interface (inlet: e and outlet: s), A the 2-butanone, and E is the enhancement factor (equal to 1 when there is no reaction in the liquid phase).

The liquid side mass transfer coefficient k_L was deduced from the values of k_La and a.

2.3. Analyses

2.3.1. Gas phase analyses

CO_2 concentrations in the gas phase (inlet and outlet) were measured with an IR analyser type Beryl 100 from COSMA. 2-Butanone concentrations in the gas phase (inlet and outlet) were indirectly measured after trapping it in a 2,4-dinitrophenylhydrazine (2,4-DNPH) solution. Indeed, the trapping yields for 2-butanone exceed 99%. This method consists of the reaction between 2-butanone and 2,4-DNPH, giving an hydrazone which is then analysed by HPLC (C18, mobile phase composed of 80% methanol and 20% water, UV detection for a wavelength of 365 nm).

2.3.2. Liquid phase analyses

The method used to measure the liquid 2-butanone concentration is again based on the reaction of the 2-butanone with the 2,4-DNPH. The quantity of carbon dioxide transferred in the liquid phase is deduced from the measure of carbonates in the solution (Norm AFNOR NF T 90-036, July 1977).

As concerns the pH and the temperature, continuous measurements were made with specific probes.

3. Results and discussion

3.1. Pressure drop

Pressure drop is one of the most important design criterions for a contactor. It allows the quantification of the dissipated power and is also a decisive factor for the estimation of the efficiency of the contactor. It depends on the liquid and gas flow rates, type of fluid [14,45] and internal geometry.

3.1.1. Pressure drop in horizontal and vertical downward flow

Figs. 2 and 3 show a comparison of pressure drop generated by three types of contactor (empty pipe, Lightnin SM and the CoReC) placed in the horizontal and the vertical downward flow positions. As it can be seen, the configuration does not seems to have any influence on pressure drop values in these reactors. Meanwhile, pressure drop in horizontal flow is slightly greater certainly because, in this configuration, gravitational effects make more difficult the establishment of a dispersed spray, whereas in vertical downward flow, gravity force plays a positive role. Comparing the three contactors, pressure drop in the empty pipe is lower than the one in the CoReC, which is far lower than the one of Lightnin SM [21]. It seems obvious that the more important the void fraction is, the lower the pressure drop is.

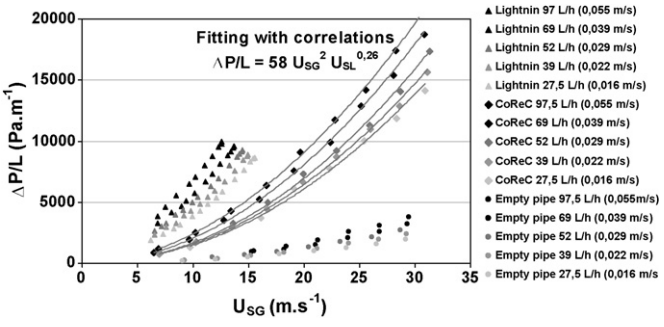

Fig. 2. Evolution of pressure drop ΔP vs. superficial gas and liquid velocities for the CoReC, the empty pipe and the Lightnin SM in VD flow configuration.

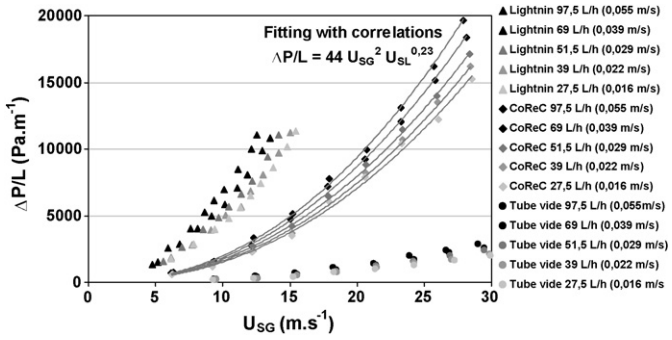

Fig. 3. Evolution of pressure drop ΔP vs. superficial gas and liquid velocities for the CoReC, the empty pipe and the Lightnin SM in H flow configuration.

3.1.2. Pressure drop in vertical upward flow

In vertical upward flow, the flow behaviour is different of the one in the other two configurations. As shown in Fig. 4, for $U_{SG} < 20\,m\,s^{-1}$, the liquid prevents the gas circulation from the bottom to the top of the contactor by forming a thick layer. The liquid has to overcome the gravity force to flow out, which leads to pressure drops greater than the ones obtained in the other configurations. For higher superficial gas velocities ($U_{SG} > 20\,m\,s^{-1}$), pressure drop follows the same behaviour as in the other two configurations. The liquid is dispersed into small drops which are driven by the gas flow, and a thin layer can be observed along the pipe wall. In the empty pipe, the same behaviour is observed. At the opposite of the behaviour encountered in experiments lead with Lightnin SM [21], which have a plain structure, the liquid flows up the pipe in the CoReC, even for small gas velocities,.

3.1.3. Pressure drop correlation

The experimental results show that pressure drop depends not only on the superficial gas velocity but also on the superficial liquid velocity. To take the influence of both velocities on the pressure drop into account, the correlation (10) is proposed:

$$\Delta P = A U_{SL}^{\alpha} U_{SG}^{\beta} \quad (10)$$

A, α and β are the parameters to be identified for each configuration (see Table 3).

Table 3 shows that the coefficient A is different for each configuration, this is mostly due to the gravity force that does not play exactly the same role in each flow configuration (positive effect in VD flow, negative effect in VU flow, stratification effect in H flow). Nevertheless, values are close except for the VU flow configuration when $U_{SG} < 20\,m\,s^{-1}$. α is slightly different and β is the same for the three configurations except for the vertical upward at superficial gas velocities lower than $20\,m\,s^{-1}$. The values of the exponent α are very small compared to β. This indicates that the gas velocity has a more important effect than the liquid velocity on pressure drop. These results can be compared to the literature where, in two-phase flow, in SM used with a liquid continuous phase, the exponent relative to U_{SL} is greater than the one relative to U_{SG} [22]. So, it can be deduced that the behaviour of the CoReC, referring to the respective influences of the superficial fluid velocities, is reversed when the operating conditions are reversed.

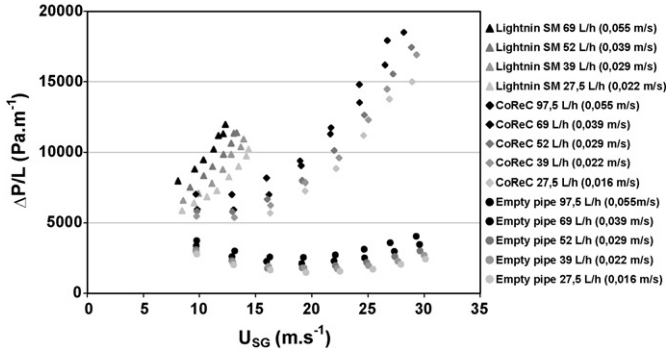

Fig. 4. Evolution of pressure drop ΔP vs. superficial gas and liquid velocities for the CoReC, the empty pipe and the Lightnin SM in VU flow configuration.

Table 3
Pressure drop correlation parameters, $\Delta P = A U_{SL}^{\alpha} U_{SG}^{\beta}$

	A	α	β	Fitting (%)
Horizontal	58	0.26	2	6
Vertical downward	44	0.23	2	5
Vertical upward				
$U_{SG} < 20\,m\,s^{-1}$	1480	0.25	0.9	10
$U_{SG} > 20\,m\,s^{-1}$	57	0.33	2	

Table 4
Comparison of the pressure drops obtained in the different contactors for $3 < U_{SG} < 15\,m\,s^{-1}$ and $0.01 < U_{SL} < 0.06\,m\,s^{-1}$

Pressure drop, $\Delta P/L$ (Pa m^{-1})	
Empty pipe	400–4000
Lightnin SM	1000–12,000
Sulzer SMV$_4$	10,000–50,000
CoReC	500–5000

3.1.4. Comparison with conventional static mixers

In Figs. 2–4 are also represented the evolution of pressure drop ΔP versus superficial gas and liquid velocities for Lightnin SM in the three configurations (H, VD and VU). Whatever the flow direction, the pressure drops observed in the different contactors are of the same order, and summarised in Table 4. The values obtained in the CoReC are largely lower than those generated by Lightnin and Sulzer SMV$_4$ SM which can reach 50,000 Pa/m in the same range of superficial gas and liquid velocities, and are logically higher than those observed in the empty pipe. Table 5 presents the values of the parameters of the correlation and the fitting between the experimental pressure drops measured for the different contactors (CoReC, Lightnin,

Table 5
Comparison of the pressure drop correlation parameters in vertical downward flow for the different contactors

	A	α	β	Fitting (%)
CoReC ($5 < U_{SG} < 30\,m\,s^{-1}$)	58	0.26	2	6
Lightnin SM ($2 < U_{SG} < 15\,m\,s^{-1}$)	573	0.52	1.6	5
Sulzer SMV$_4$ ($5 < U_{SG} < 12\,m\,s^{-1}$)	6185	0.30	1.68	10
Empty pipe ($5 < U_{SG} < 30\,m\,s^{-1}$)	21	0.54	2.02	7

Sulzer SMV_4 and empty pipe) in VD flow and the correlation associated. The parameter A, which takes into account various parameters as friction, gravity or inertia forces, is greater in Sulzer (6185) and Lightnin SM (573) and logically lower in the empty pipe (21) than in the CoReC (58). α and β slightly differ in the four reactors; β in the CoReC is equal to β in the empty pipe. These results can be explained by the "aerated" structure of the CoReC (high void fraction), which offers less resistance to the fluid flows than the other SM.

3.1.5. Friction factor

The friction factor f is an important parameter since its knowledge enables to evaluate the pressure drop generated by the contactor. In one phase flow (gas only), pressure drop can be correlated by a power law type equation (11):

$$\Delta P = \alpha U_G^{\beta} \tag{11}$$

The friction factor f is deduced from Darcy equation (12):

$$f = \frac{\Delta P L \rho_G U_{SG}^{\beta}}{2 D_i} \tag{12}$$

L is the contactor length and ρ_G the gas density and D_i is the pipe internal diameter.

By identifying the experimental pressure drops in one phase flow to those calculated with Darcy equation, the friction factor can easily be calculated. The values found for the different contactors are reported in Table 6. In the CoReC, the friction factor decreases with the superficial gas velocity to tend toward a plateau value of 0.16. It can be considered as constant in fully turbulent flow. This value is greater than the one obtained in an empty pipe but lower than the values obtained for Lightnin and Sulzer SMV_4 SM.

In 1982, Pahl and Muschelknautz [41] have also shown that SM generate a pressure drop strongly dependent on the geometry of the mixing elements. The greater the space left for the fluid flow is, the lower the pressure drop is. This hypothesis is fulfilled in our experiments as regard to the structures of Sulzer SMV_4 SM (78% void fraction) composed of embossed plates stacked in layers and Lightnin SM (87% void fraction) composed helical elements whereas the void fraction in the CoReC is 97.5%.

3.2. Volumetric interfacial area

Gas–liquid interfacial area a ($m^2\ m^{-3}$ of reactor) is an important parameter for the design of gas–liquid reactors in which dispersion occurs because it influences volumetric mass transfer coefficients $k_L a$ and $k_G a$.

Table 6
Comparison of the friction factors obtained in the different contactors for $3 < U_{SG} < 15\ m\ s^{-1}$ and $0.01 < U_{SL} < 0.06\ m\ s^{-1}$

Friction factor	
Empty pipe	0.02
Lightnin SM	0.30
Sulzer SMV_4	1.85
CoReC	0.16

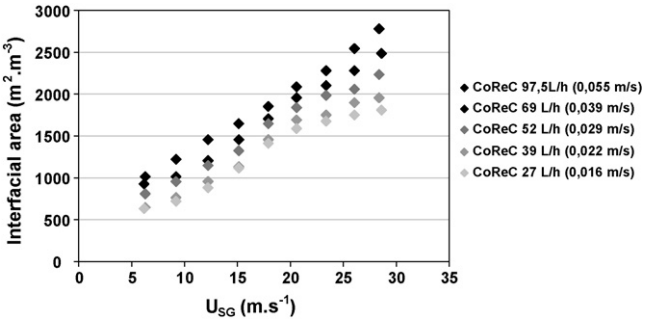

Fig. 5. Evolution of volumetric interfacial area a vs. superficial gas and liquid velocities for the CoReC in VD flow configuration.

Note. The determination of the interfacial area and the gas side mass transfer parameters needs some hypotheses to be fulfilled: first, the rapid reaction regime criteria which is given by the condition $Ha > 5$ [23], secondly, the pseudo-first-order reaction criteria which is given by the condition $Ha < E_i/2$ [24]. During our experiments, we have satisfied the conditions required for the determination of the interfacial area with the CO_2/NaOH system. We have verified that the chemical reaction used is fast (Ha number is always greater that 25) and irreversible of the pseudo-first order (Ha/E_i is always lower than 0.01).

3.2.1. Interfacial area in horizontal and vertical downward flow

Figs. 5 and 6 show a comparison of interfacial areas in the CoReC in H and VD flow configurations. VD configuration leads to volumetric interfacial areas higher than H configuration (600–2700 $m^2\ m^{-3}$ against 150–1900 $m^2\ m^{-3}$). This can be explained the gravity force which plays a positive role in VD configuration whereas it constitutes a brake to the liquid flow in H configuration.

3.2.2. Interfacial area in vertical upward flow

In vertical upward flow, the behaviour is different than in the two others configurations. As shown in Fig. 7, for $U_{SG} < 20\ m\ s^{-1}$, the liquid phase prevents the gas phase from circulating upward by forming a thick layer. The liquid has to overcome the gravity force to flow out, so that agitation in the pipe is higher and, as a result interfacial areas are higher than in the other configurations (about 1200 $m^2\ m^{-3}$ against 150–600 in

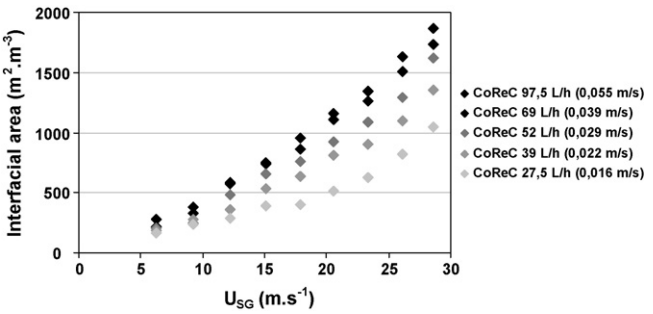

Fig. 6. Evolution of volumetric interfacial area a vs. superficial gas and liquid velocities for the CoReC in H flow configuration.

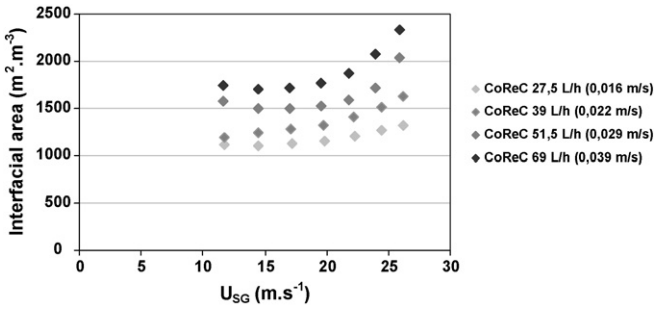

Fig. 7. Evolution of volumetric interfacial area a vs. superficial gas and liquid velocities for the CoReC in VU flow configuration.

H and VD configurations, respectively). For higher superficial gas velocities, interfacial areas tends to have the same behaviour as in the other two other configurations, the liquid is dispersed in small droplets which create a high exchange surface. Maximal values are lower than those obtained in VD configuration.

3.2.3. Volumetric interfacial area correlation

Experimental results show that the interfacial area depends not only on the superficial gas velocity but also on the superficial liquid velocity. To take the influence of the liquid and gas superficial velocities on the interfacial area into account, the correlation (13) is proposed:

$$a = AU_{SL}^{\alpha}U_{SG}^{\beta} \quad (13)$$

A, α and β are the parameters to be identified for each configuration.

The different parameters relative to the configuration and the fitting between experimental data and correlation are given in Table 7. As expected, the values of α are smaller than the ones of β. This indicates that the gas velocity has a more important effect than the liquid velocity on volumetric interfacial area. Otherwise, it can be noticed that the more the coefficient A increases, the more the exponents α and β decrease. Evolution of the coefficient A can be related to the hydrodynamic behaviour of the reactor: A increases with turbulence and drop formation. Moreover, the α to β ratio increases from the H configuration to the configuration VD, and from the VD configuration to the VU configuration, reflecting the increasing influence of the liquid.

3.2.4. Comparison with conventional contactors

As shown in Table 8, the values obtained in the CoReC are largely higher than those encountered in the classical processes in which the gas is the continuous phase (like PT or spray columns). Moreover, they can be three times higher than those generated by Lightnin SM [21], and far greater than those

Table 7
Volumetric interfacial area correlation parameters, $a = AU_{SL}^{\alpha}U_{SG}^{\beta}$

	A	α	β	Fitting (%)
Horizontal	113	0.55	1.32	10
Vertical downward	622	0.33	0.72	6
Vertical upward	4560	0.28	0.53	6

Table 8
Comparison of the volumetric interfacial area a obtained in the CoReC and conventional gas–liquid contactors ($U_{SG} < 15\,m\,s^{-1}$ and $U_{SL} < 0.06\,m\,s^{-1}$)

Type of gas–liquid contactor	a ($m^2\,m^{-3}$ of reactor)
Packed towers	10–350
Spray towers	10–100
Structured packing [28]	10–410
High velocity spray columns [39]	50–200
Empty pipe	50–700
Lightnin SM	100–1000
Sulzer SMV_4	1200–3700
CoReC	100–2700

obtained in the empty pipe. This can be explained by the high energy dissipation inside the CoReC. Nevertheless, they are lower than those encountered in Sulzer SMV_4 SM, which can reach about $3700\,m^2\,m^{-3}$ in the same range of gas and liquid superficial velocities.

In counter-current conditions, in conventional dumped packed columns, geometric interfacial area generally equals about 100–300 $m^2\,m^{-3}$ (involving low L/G operating ratios, about 1–3), and the effective wet interfacial area is rarely as high as the geometric value. This is not the case of structured packing operating in counter-current flows, where geometric interfacial areas can reach values ranging from 250 up to $750\,m^2\,m^{-3}$ [25,26]. In 2004, Raynal et al. used a high geometric area structured packing ($410\,m^2\,m^{-3}$) in co-current flows and found that the effective wet interfacial area can reach the geometric value if the liquid velocity is sufficient. They concluded that in order to take advantage of the high geometric area given by structured packings, a minimum of L/G ratio is required (greater than 20 in their case). This value is high in comparison with the common range for the absorption applications, and especially with the ratios implemented in this study.

3.3. Gas side volumetric mass transfer coefficient k_Ga

The hypothesis of no gas-side resistance is commonly accepted for co-current downward trickle flow in random-packed columns [27]. Fig. 8 shows an example of graph, which must be used to determine k_Ga. As it can be observed, the intercept is negative which does not allow us to quantify k_Ga. This

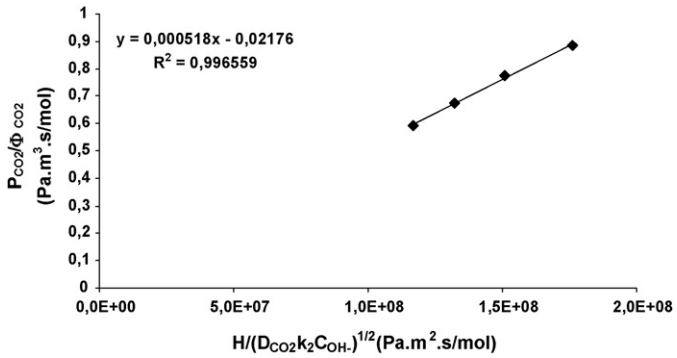

Fig. 8. P_{CO_2}/Φ_{CO_2} vs. $[H/(\sqrt{D_{CO_2}k_2C_{OH^-}})]$ plot for U_{SG}=20 $m\,s^{-1}$ and U_{SL}=0.039 $m\,s^{-1}$ in VD flow configuration.

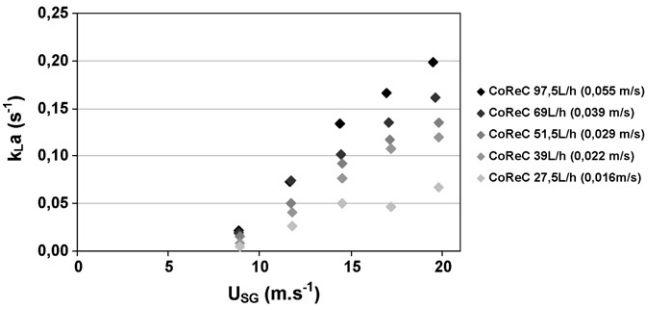

Fig. 9. Evolution of volumetric mass transfer coefficient k_La vs. superficial gas and liquid velocities for the CoReC in the H flow configuration.

is due to the accuracy of this method. It seems that the intercept is much less than the measured values of P_{CO_2}/Φ_{CO_2}. Nevertheless, it can be asserted that the intercept is not of the same order of magnitude as P_{CO_2}/Φ_{CO_2}, or in other words that mass transfer is not limiting by the gas side, and that the gas resistance can be neglected.

3.4. Liquid side volumetric mass transfer coefficient k_La

Few experimental data on mass transfer coefficients in SM or structured packings are available in the literature in comparison with those for other gas–liquid reactors (bubble columns, stirred vessels). In the VU configuration, the method used for the determination of k_La has shown its limit in the saturation of the liquid solution by 2-butanone. This inconvenient makes the quantification of 2-butanone absorbed in the liquid phase impossible. Consequently, only the results on VD and H configurations are described as a function of superficial liquid and gas velocities in Figs. 9 and 10. As it can be seen, k_La increases with increasing liquid and gas velocities, like volumetric interfacial area.

VD configuration leads to better k_La coefficients than H configuration. Promising values, up to $0.20\,s^{-1}$, have been measured whatever the flow configuration is. As a comparison, k_La found in PT varies between $2.5 \times 10^{-3}\,s^{-1}$ and $0.035\,s^{-1}$ [27].

3.4.1. k_La correlations

Experimental results show that k_La depends not only on the superficial gas velocity but also on the superficial liquid velocity. To take the influence of the liquid and gas superficial velocities

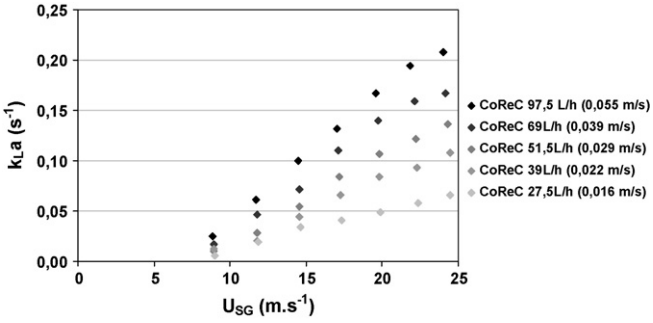

Fig. 10. Evolution of volumetric mass transfer coefficient k_La vs. superficial gas and liquid velocities for the CoReC in the VD flow configuration.

Table 9
Volumetric mass transfer coefficient correlation parameters, $k_La = AU_{SL}^{\alpha}U_{SG}^{\beta}$

	A	α	β	Fitting (%)
Horizontal ($U_{SG} < 24\,m\,s^{-1}$)	0.02	0.51	1.15	15
Vertical downward ($U_{SG} < 22\,m\,s^{-1}$)	0.01	0.93	1.83	6

on the k_La into account, the correlation (14) was proposed:

$$k_La = AU_{SL}^{\alpha}U_{SG}^{\beta} \quad (14)$$

A, α and β are the parameters to be identified for each configuration.

The parameters relative to the different configurations and the fitting between experimental data and correlation are given in Table 9. Again, the values of the exponent α are smaller than the ones of β, testifying of the more important effect of the gas velocity on k_La. Moreover, it can be observed that, if A is greater in the H configuration than in the VD configuration, the exponents α and β are smaller in this flow configuration.

3.4.2. Comparison with conventional contactors

As shown in Table 10, the values obtained in the CoReC are much higher than those met in classical PT in which the gas is the continuous phase, and can be twice higher than those generated by Lightnin SM (15×10^{-2} against $7 \times 10^{-2}\,s^{-1}$ in the same operating conditions). Nevertheless, they are lower than those encountered in Sulzer SMV_4 SM, which can reach about $20 \times 10^{-2}\,s^{-1}$ in the same range of superficial gas and liquid velocities. As a comparison, k_La found in random PT varies between 0.01 and $0.06\,s^{-1}$ [27]. k_La found in structured PT are expected to be higher depending on the geometric characteristics of the packing elements. As an example, Raynal et al. [28] found k_La values ranging from $0.15\,s^{-1}$ up to $0.25\,s^{-1}$ with their packing made of smooth stainless sheets, but at high L/G ratios.

3.5. Prediction of the film mass transfer coefficient k_L

The values of the liquid-side mass transfer coefficient k_L can been estimated from the values of k_La and specific interfacial area a, with Eq. (15):

$$k_L = \frac{k_La}{a} \quad (15)$$

Table 10
Comparison of the k_La obtained in the CoReC and conventional gas–liquid contactors ($U_{SG} < 15\,m\,s^{-1}$ and $U_{SL} < 0.06\,m\,s^{-1}$)

Type of gas–liquid contactor	k_La (s^{-1})
Packed towers	4×10^{-4} to 7×10^{-2}
Bubble columns	5×10^{-3} to 20×10^{-2}
Venturis	8×10^{-2} to 25×10^{-2}
Empty pipe	5×10^{-4} to 5×10^{-2}
Lightnin SM	3×10^{-2} to 7×10^{-2}
Sulzer SMV_4	2×10^{-2} to 20×10^{-2}
CoReC	7×10^{-3} to 15×10^{-2}

Values between $5 \times 10^{-6}\,m\,s^{-1}$ and $8 \times 10^{-5}\,m\,s^{-1}$ were obtained for the different flow configurations. k_L increases with the superficial gas velocity but slightly depends on the superficial liquid velocity. The comparison of these values to the ones obtain in classical packed towers ($5 \times 10^{-5} < k_L\ (m\,s^{-1}) < 5 \times 10^{-4}$) shows that k_L measured in the CoReC is about 10 times lower. This result can be explained by the rigidity of the drop wrapping. Surface renewal and rigid body models show that the more rigid a particle wrapping is, the smaller the k_L value is.

4. Conclusion

The aim of this study was to characterise the hydrodynamics and the mass transfer in a new type of gas–liquid contactor, the CoReC, in different flow configurations (VD, H and VU). Pressure drop, volumetric interfacial area and mass transfer coefficients k_La and k_Ga were measured for the three flow configurations, at superficial gas velocities ranging from 5.6 to $28\,m\,s^{-1}$ and superficial liquid velocities varying from 0.016 to $0.055\,m\,s^{-1}$. The influences of both liquid and gas velocities were demonstrated. It has been shown that, for a given liquid velocity, pressure drop, interfacial area and liquid-side volumetric mass transfer coefficient increase with an increasing superficial gas velocity. Nevertheless, the superficial liquid velocity has little influence on these parameters. As regards all the results, the CoReC seems to be the best energy consumption/transfer efficiency compromise, in comparison with classical SM and classical structured PT.

At last, the flow configuration is an important parameter to take into account. The position VU configuration proved to be very efficient but constraining in terms of energy costs and running conditions. At low fluid velocities, the H configuration leads to flow stratification, which is not appropriate for mass transfer. The VD configuration seems to be the most convenient because it is easy to use, provides low pressure drops and good mass transfer coefficients.

As a conclusion, the CoReC appears to be a new low investment and operating cost alternative to conventional contactors for the treatment of large gas volumes with low concentrations of pollutants. Compared with PT, which can provide the same range of values, the operating conditions in the CoReC are far less drastic and the dimensions of the apparatuses are far smaller than those used in traditional processes.

References

[1] L. Bravo, J.A. Rocha, J.R. Fair, Mass transfer in Gauze packings, Hydrocarbon Process. (1985) 91–95.

[2] P. Bomio, K. Breu, Structured packings in high pressure absorption columns, Hydrocarbon Technol. Int. Quart. 94/95 (1995) 99–104.

[3] J.R. Fair, A.F. Seibert, M. Behrens, P.P. Saraber, Z. Olujic, Structured packing performance-experimental evaluation of two predictive models, Ind. Eng. Chem. Res. 39 (2000) 1788–1796.

[4] J.P. Ballaguet, C. Barrere-Tricca, C. Streicher, Improvements to tail gas treatment process, Petrol. Technol. Quart. (2003) 109–115.

[5] De Vos, Un mélangeur statique aux applications multiples, Informations Chimie 109 (1972) 109–123.

[6] A. Cybulski, K. Werner, Static mixers—criteria for applications and selection, Int. Chem. Eng. 26 (1) (1986) 171–180.

[7] G. Rader, M. Mustakis, F. Grosz-Roll, W. Maugweiler, Better absorption? Try a static mixer, Chem. Eng. (1989) 137–142.

[8] J.R. Baker, Motionless mixers stir up new uses, Chem. Eng. Progr. 876 (1991) 32–38.

[9] J.R. Bourne, H. Maire, Micromixing and fast chemical reactions in static mixers, Chem. Eng. Process. 30 (1991) 23–30.

[10] F.A. Streiff, J.A. Rogers, Don't overlook static-mixer reactors, Chem. Eng. (1994) 76–81.

[11] E. Germain, F.A. Streiff, J.E. Juvet, Les mélangeurs statiques, des réacteurs simples et efficaces, Informations Chimie 374 (1996) 141–147.

[12] R. Billet, Packed Towers in Processing and Environmental Technology, Weinheim, Germany, 1995.

[13] K.J. Myers, A. Baker, D. Ryan, Avoid agitation by selecting static mixer, Chem. Eng. Progr. (1997) 28–38.

[14] C. Traversay, R. Bonnard, C. Adrien, F. Luck, Static mixer: a reactor for the ozone process., in: Proceedings of the International Specialised Symposium IOA—Fundamental and Engineering Concepts for Ozone Design, Toulouse, 2000, pp. 155–161.

[15] A.M. Al Taweel, J. Yan, D. Odebra, H.G. Gomaa, Using in-line static mixers to intensify gas–liquid mass transfer processes, Chem. Eng. Process. 44 (12) (2005) 1285–1295.

[16] P.Y. Le Strat, M. Cot, J.P. Ballaguet, J.L. Ambrosino, C. Streicher, J.P. Cousin, New redox process successful in high pressure gas streams, Oil Gas J. 11 (2001) 46–54.

[17] R. Pohorecki, W. Moniuk, Kinetics of reaction between carbon dioxide and hydroxyle ions in aqueous electrolyte solutions, Chem. Eng. Sci. 43 (1988) 1677–1684.

[18] A. Laurent, 1975. Etude de l'hydrodynamique et de transfert de matière dans une colonne à garnissage. Simulation de son fonctionnement à contre-courant par des modèles expérimentaux de laboratoire lors d'une absorption gaz-liquide avec réaction chimique. PhD thesis. INPL, Nancy, France.

[19] C.R. Wilke, P. Chang, Correlation of diffusion coefficients in dilute solution, AIChE J. 1 (1955) 264–270.

[20] M. Roustan, Transferts gaz-liquide dans les procédés de traitement des eaux et des effluents gazeux, Tech. & Doc. Lavoisier, Paris, 2003.

[21] A. Couvert, C. Sanchez, I. Charron, A. Laplanche, C Renner, Static mixers with a gas continuous phase, Chem. Eng. Sci. 61 (11) (2006) 3429–3434.

[22] A. Heyouni, M. Roustan, Z. Do-Quang, Hydrodynamics and mass transfer in gas–liquid flow though static mixers, Chem. Eng. Sci. 57 (2002) 3325–3333.

[23] D.W. Van Krevelen, P.J. Hoftijzer, Kinetics of gas liquid reactions. Part I. General theory, Recueils Trav. Chim., Pays Bas. 67 (1948) 563.

[24] A. Badssi, 1984. Absorption gaz–liquide avec réaction chimique: Détermination des coefficients de transfert de matière et de l'aire interfaciale des colonnes à plateaux. PhD thesis. Institut National Polytechnique de Toulouse, France.

[25] P.A. Nawroski, Z.P. Xu, K.T. Chuang, Mass transfer in structured corrugated packing, Can. J. Chem. Eng. 69 (1991) 1336–1343.

[26] M. Dragan, A. Friedl, M. Harasek, S. Dragan, I. Simiseanu, Measuring the effective mass transfer area of a Mellapack 750Y structured packing, in: Proceedings of the 14th International Congress of Chemical and Process Engineering, CHISA, 27–31 August, 2000, p. 2000.

[27] J.-C. Charpentier, Mass transfer rates in gas liquid absorbers and reactors, in: T.B. Drew, G.R. Cokelet, J.W. Hoopes, T. Vermeulen (Eds.), Advances in Chemical Engineering, vol. 11, Academic Press, New York, 1981, pp. 1133–1134.

[28] L. Raynal, J.-P. Ballaguet, C. Barrere-Tricca, Determination of mass transfer characteristics of co-current two-phase flow within structured packing, Chem. Eng. Sci. 59 (2004) 5395–5402.

[30] E. Brunazzi, A. Paglianti, S. Pintus, A capacitance probe and a new model to identify and predict the capacity of columns equipped with structured packings, Ind. Eng. Chem. Res. 40 (2001) 1205–1212.

[31] O.N. Cavatorta, U. Bohm, A.M. Chiappori de del Giorgio, Fluid-dynamic and mass-transfer behavior of static mixers and regular packing, AIChE J. 45 (5) (1999) 938–948.

[32] C. Chen, 1995. Dispersion and coalescence in static mixers. PhD thesis. Technical University of Nova Scotia, Canada.

[33] P.V. Danckwerts, Gas–Liquid Reactions, McGraw-Hill Editions, New York, 1970.
[34] V.J. Dang, M.-H. Manero, M. Roustan, Absorption of volatile organic compounds in a tower packed with a structured packing. I. Hydrodynamic study, Entropie 34 (209) (1998) 3–10.
[35] V.J. Dang, M.-H. Manero, M. Roustan, Absorption of volatile organic compounds in a tower packed with a structured packing. II. Mass transfer, Entropie 34 (209) (1998) 11–17.
[39] F.K. Kies, 2002. Traitement des effluents gazeux sous hautes vitesses de gaz – Cas de la colonne à gouttes transportées. PhD thesis. Université de Lyon, France.
[41] M.H. Pahl, E. Muschelknautz, Static mixers and their applications, Int. Chem. Eng. 22 (2) (1982) 197–205.
[45] Z.M. Zhu, J. Hanoon, A. Green, Use of high intensity gas–liquid mixers as reactors, Chem. Eng. Sci. 47 (9–11) (1992) 2847–2852.